A New Autofocusing Method Based on Brightness and Contrast for Color Cameras

Murat SELEK
Vocational School of Technical Sciences, Selcuk University, Konya, 42003, Turkey
mselek@selcuk.edu.tr

***Abstract*—The autofocusing is one of the most important features of imaging devices. This feature directly affects the quality of the image taken by the imaging device. Currently, many studies are being performed to improve the feature of autofocusing. In this study, we propose a method for passive autofocusing of the color cameras. This method suggested is called as the Passive Autofocusing Based-Brightness and Contrast (PA Based-BC). According to this method, autofocusing is performed by identifying the brightness of the R, G and B color components of the RGB image and by focusing of the camera on the brightest color component. To this end, in this study, many experiments have been conducted. The analyses of these experiments show that the contrast-based focusing made depending on the brightness gives much better results. The use of this method upgrades the focusing accuracy of the color camera up to 95%.**

***Index Terms*—CCD image sensors, digital images, focusing, image color analysis, image processing.**

I. Introduction

The quality of an image taken by a camera depends on the extent to which the camera focuses on the object being photographed [1-6]. Focusing of a camera may be performed manually or automatically [6]. Autofocusing methods used in existing cameras are divided into two categories: active and passive [4], [5], [7-11]. In active autofocusing (AA), the infrared (IR) or ultrasonic waves emitted by a source embedded in the camera are reflected by the object to be photographed, and the camera focuses on the object based on the intensity of this reflection [4], [5], [8-12]. Though the AA method seems to have advantages over passive autofocusing (PA), it has some disadvantages in practice as well. In case of ultrasonic wave, the camera cannot be focused on objects behind of glass barrier because glass is a good reflector for ultrasonic wave. Besides, in case of IR waves, the presence of some other objects radiating IR waves in the displayed area may adversely affect the focusing [5], [13]. In addition, the AA has the following disadvantages:

It gets harder with increasing of the distance between the camera and the object and might be impossible beyond a certain distance [6].

It requires too much power and cameras of relatively large-sizes [8], [12], [14].

The PA methods perform focusing using the methods such as contrast, variance, correlation, histogram or thresholding obtained from the gray values of the pixels of the image [4], [7], [15-20]. From these methods, the most sensitive one for high frequency components, namely for the sharp edges of the image, is the contrast [13]. The contrast-based PA algorithms are also referred to as derivative-based ones. These algorithms perform focusing by using differences between the gray values of the pixels of the image. The most widely used contrast-based PA algorithms are: the Threshold Absolute Gradient Algorithm, the Squared Gradient Algorithm, the Brenner Gradient Algorithm, the Tenenbaum Gradient Algorithm, the Sum of Modified Laplace Algorithm, the Energy Laplace Algorithm and the Wavelet Algorithm [3], [7], [15-18], [21-26].

The objects to be displayed using the PA should be illuminated to a degree at which the needed level of contrast is arisen [27]. Otherwise, a good focusing is not possible since the details in the scene cannot be fully seen [1], [27], [28]. In PA systems, there are no limitations above-mentioned for AA. Moreover, in PA systems, good results can be obtained, especially when the object being displayed is behind a glass or in an environment where there are IR light sources. Due to this features, for autofocusing of the cameras in practice, generally the PA algorithms are used [14].

It is commonly known that as the high frequency content of an image increases, so does the contrast between the pixels of it [29-31]. In other words, images with sharply changing contrast distribution have more high-frequency components, whereas those with a smoother contrast distribution have fewer high-frequency components. Therefore, as the contrast between the pixels of an image increases, the edges get sharper [19], [20]. That is, the image becomes clearer [19], [29], [32].

Images obtained by using monochrome cameras are referred to as grayscale or black-white images. For instance, thermal cameras and black-white cameras are monochrome imaging devices. In PA systems used to perform autofocusing with such devices, the image obtained from the camera is processed by using an appropriate focusing algorithm, and the lens position which yields the clearest image is sought [25], [32-34]. The performance of the PA algorithm implemented to the image determines how successful the algorithm is.

In RGB (red, green and blue) images obtained by using color-cameras, each pixel is represented by three distinct colors such as R (Red), G (Green) and B (Blue). The combinations of these colors determine the color of the pixel. In the most frequently used 8-bit color format, each color component (R, G or B) has a value between 0 and 255.

In Fig. 1, a RGB image and its R, G and B components that have the brightness values between 0 and 255 of each obtained by using three separate color filters (red, green, and blue) are presented [35]. The separately examining of the R,

This work was supported by Selcuk University Scientific Research Projects Coordinatorship, Konya, Turkey.

Digital Object Identifier 10.4316/AECE.2016.04006

G and B components of a lot of RGB images has shown that generally the R, G and B components of an image have different brightness and contrasts. Panicker et al. indicated that it is important also its brightness as much as the contrast of an image [36]. Therefore, in this study, besides the contrast of the image, the brightness of the R, G and B components is determined.

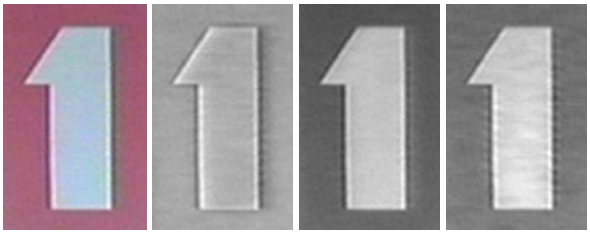

(a) (b) (c) (d)

Figure 1. (a) Color (RGB) image, (b) component R, (c) component G, (d) component B

Thus, the PA for an object being photographed is carried out in two steps: identifying the brightest color (R or G or B) component of the image and performing contrast-based focusing of the camera on the identified component. In the other words, the brightness (mean gray value) for each R, G and B color component of the field to be focused in an RGB image is calculated, and the brightest color component is used for focusing. The clearest image is sought by applying the Adaptive Squared Gradient Algorithm (ASGA) based on contrast to the color component chosen, and the lens position at which this image is obtained is referred to as the best focus position [19].

In [19], the focusing accuracy of the ASGA for thermal images being monochrome was reported to have reached 96%. In this study, we divided the PA Based-Brightness and Contrast (PA Based-BC) into two steps such as identifying the brightest component of the image, and focusing by the ASGA based-contrast of the camera on the identified component. This approach allows us to apply the PA Based-BC to the color images with the focusing accuracy of 95% as shown the Table IV in Section V.

II. Obtaining RGB Images Using CCD Array with Bayer Color Filter

Most of the digital cameras that use CCD or CMOS image sensors use RGB color model. The RGB color space consists of three main color components; namely, R, G and B (Fig. 2.a). Therefore, each element of the CCD array is designed in such a way to perceive only one component of the RGB color model. To do this, in digital cameras, the surface of CCD array is covered with Bayer filter. As it is shown in Fig. 2.b, Bayer filter is a mosaic color filter array that makes it possible for each component of the CCD array to perceive the R, G and B color components [37-40]. In this filter, in each 4-pixel square CCD area, there are one R, one B and 2G filters.

Since human eye is more sensitive to green, two G filters are used [37], [38], [40]. The image obtained from the CCD array with the Bayer filter is formed in the form of a mosaic [37-40]. To obtain a high resolution color image, as seen in Fig. 3, the value of the color missing in each pixel is completed by using the one of the interpolation methods such as piecewise constant, linear, polynomial and spline [37], [38]. In this way, a high quality color image is obtained.

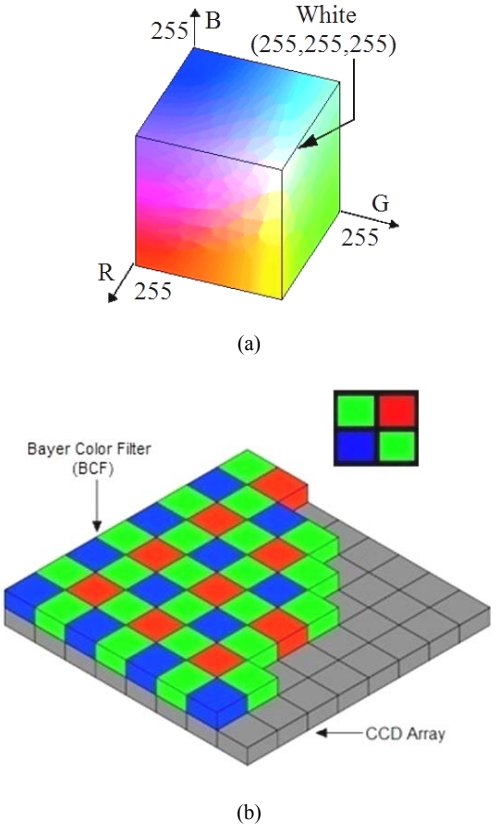

Figure 2. (a) RGB color space, (b) a Bayer Color Filter Array

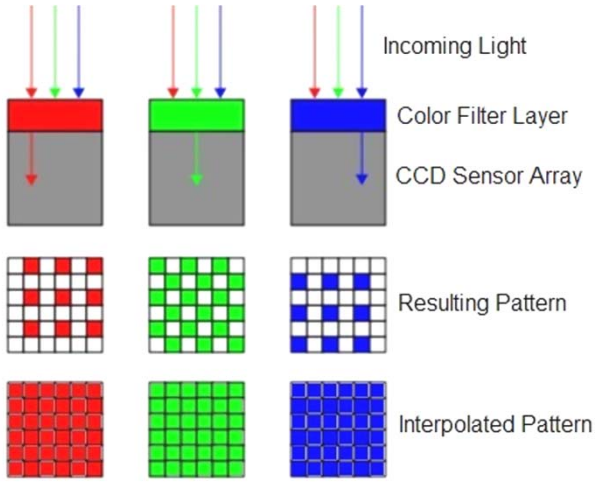

Figure 3. Obtaining the interpolated RGB image

As seen in Fig. 3, in the RGB color model, each of the R, G and B components of a color image is referred to as a matrix, where m and n are the number of rows and the columns of a color matrix, and r, g and b are the values of R, G and B color matrixes, respectively.

$$R=\begin{bmatrix} r_{11} & .. & r_{1n} \\ .. & .. & .. \\ r_{m1} & .. & r_{mn} \end{bmatrix} G=\begin{bmatrix} g_{11} & .. & g_{1n} \\ .. & .. & .. \\ g_{m1} & .. & g_{mn} \end{bmatrix} B=\begin{bmatrix} b_{11} & .. & b_{1n} \\ .. & .. & .. \\ b_{m1} & .. & b_{mn} \end{bmatrix}$$

III. Using of the Passive Autofocusing Based-Brightness and Contrast (PA Based-BC) in Focusing of the RGB Images

The block schema of an RGB camera is given in Fig. 4.

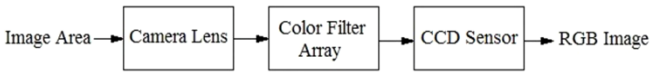

Figure 4. Block diagram of a RGB camera with Color Filter Array (CFA)

As it is well known, focusing the camera on an object is the obtaining the distance between the lens and CCD image sensor providing the best photographing of the object [7], [8], [21], [22]. The connection between the object and CCD sensor is shown in Fig. 5.

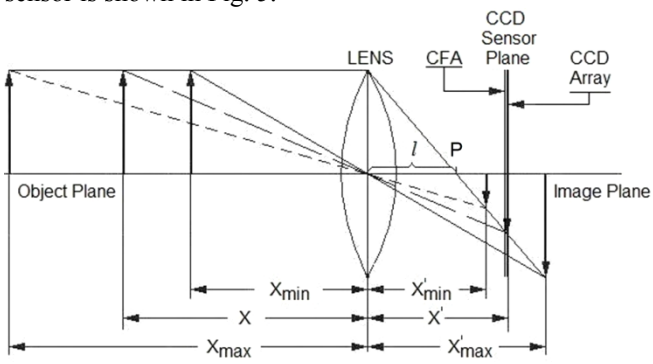

Figure 5. The focal plane of a RGB camera with CFA

In order to get an image of an object, the distance X between the object and lens and the distance X' between CCD Sensor Plane and lens are determined by the conditions $X_{min} \le X \le X_{max}$ and $X'_{min} \le X' \le X'_{max}$, respectively [14]. According to the Gaussian lens law, the optimum value (X'_{opt}) of X' providing to take a sharp image is determined by Formula (1) given below [6], [13], [19].

$$X'_{opt} = \frac{X \times l}{X - l} \tag{1}$$

In this formula, l is the focus distance of the lens. Additionally, in order to obtain the sharp image, Formula (1) must provide the following condition [19]:

$$\left| X' - X'_{opt} \right| \approx 0 \tag{2}$$

As it is well known, to get a clear image, with increasing the distance between the object and the lens, the distance of the lens from CCD array (the position in the image plane) must be properly decreased. To fix the lens in the optimal position in the focal plane, an autofocusing algorithm that controls the stepper motor which moves the lens is used.

The stepper motor control is performed in two steps in the PA Based-BC suggested by this study. The first, the brightness $\overline{R}$, $\overline{G}$ and $\overline{B}$ of the color components of the field to be focused are calculated by (3), (4) and (5), respectively. The color matrix with the highest brightness is selected as the focusing matrix F given by (6).

$$\overline{R} = \frac{1}{m \times n} \sum_{i=1}^{m} \sum_{j=1}^{n} r_{i,j} \tag{3}$$

$$\overline{G} = \frac{1}{m \times n} \sum_{i=1}^{m} \sum_{j=1}^{n} g_{i,j} \tag{4}$$

$$\overline{B} = \frac{1}{m \times n} \sum_{i=1}^{m} \sum_{j=1}^{n} b_{i,j} \tag{5}$$

$$F = \begin{bmatrix} f_{11} & .. & f_{1n} \\ .. & .. & .. \\ f_{m1} & .. & f_{mn} \end{bmatrix} \tag{6}$$

The second step of the focusing is based on (7) given in [19]. In this formula, $f_{i,j}$ is the gray value of (i,j) elements of the focus matrix F.

Note that the ASGA given in (7) is a focusing algorithm based on contrast that can successfully adapt itself to thermal images with different resolutions. In [19], it has been shown that the focusing accuracy of the algorithm might significantly be increased up to 96% by using the optimal distance k between the pixels being compared. In Table I the most of frequently used image resolutions and the values of k corresponding to them are given [19].

Table I. The Values of K for Different Resolutions of Thermal Images

Resolution	k
60×80	1
120×160	1
240×320	1
480×640	2
480×720	2
768×1024	3
960×1280	3
1200×1600	4

After the k value that matches the resolution of the camera is selected, the focus value (FV) for an image is calculated using the following formula.

$$FV = \frac{1}{m \times n} \sum_{i=1}^{m} \sum_{j=1}^{n} (f_{i+k,j} - f_{i,j})^2 + (f_{i,j+k} - f_{i,j})^2 \tag{7}$$

To get an optimal image of an object, the lens is drawn near to the CCD sensor array plane starting from a certain distance. In every $s \ge 1$ step an image is taken and FV_s focus value for this image is calculated using (7). This process goes on until the state of $FV_s - FV_{s-1} < 0$ is reached, and FV_{s-1} is taken as the optimal focus value [13], [27], [41].

IV. Experimental Setup and Materials

In this study, the PA procedure was carried out for images of the format 720×480 that were taken by the Balitech BL-344D RGB CCD camera with image capturing card. To perform our tests in this study, a computer with the Intel Core 2 Duo processor (2M Cache, 1.8 GHz, 4GB RAM) was used. The experimental setup used for this purpose is given in Fig. 6.

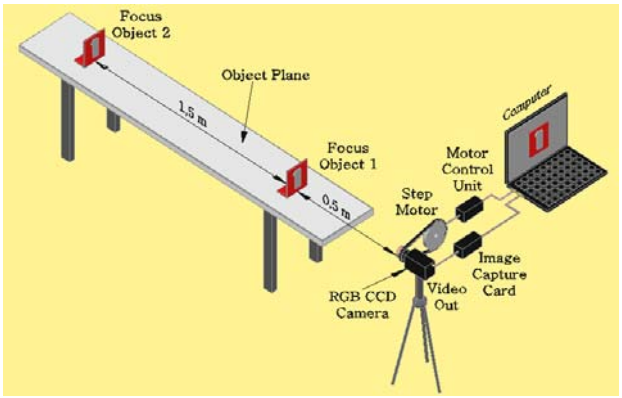

Figure 6. The experimental setup of autofocusing of RGB CCD camera

Figure 7. 5 Different patterns used in focus practices

As it is seen in Fig. 6, the experimental setup consists of an RGB CCD camera, a stepper motor, an image capturing card, a motor control unit and a computer. The distance between the lens and the CCD sensor array plane ($X^{'}$) of the camera is controlled using a stepper motor. As noted earlier, the lens is drawn near to the CCD sensor array plane starting from the position that is the furthest from CCD sensor array plane. An image is taken in every step of the lens. This process goes on until the optimal focus value is determined. The focused objects were placed at a distance of 0.5m and 2m from the camera on the object plane in the experiments. In these experiments, 5 different patterns having a width of 10cm and a height of 20cm were used (Fig. 7).

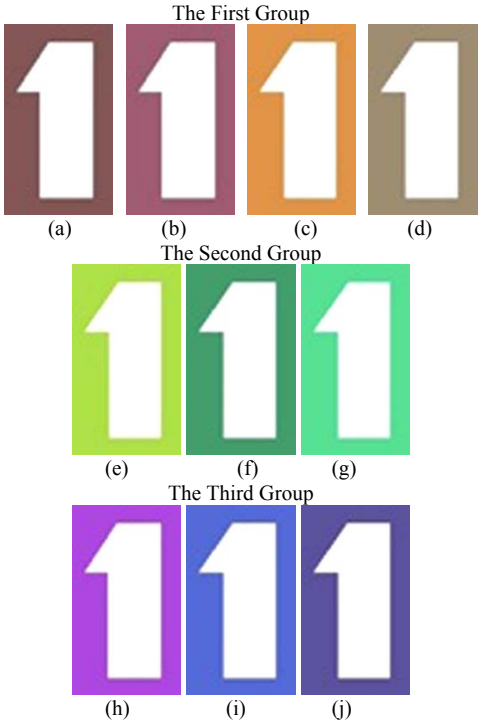

Figure 8. The colors of test objects: (a) Chocolate 2, (b) Navajo White 4, (c) Light Salmon 4, (d) Pale Violet Red 4, (e) Yellow Green, (f) Sea Green 3, (g) Sea Green, (h) Dark Orchid 3, (i) Royal Blue 3, (j) Dark Slate Blue

TABLE II. DECIMAL VALUES OF COLORS USED

Group	Color Name	Color Component Value		
		R	G	B
Dominant R	Chocolate 2	238	118	33
	Navajo White 4	139	121	94
	Light Salmon 4	139	87	66
	Pale Violet Red 4	139	71	93
Dominant G	Yellow Green	154	205	50
	Sea Green 3	67	205	128
	Sea Green	46	139	87
Dominant B	Dark Orchid 3	154	50	205
	Royal Blue 3	58	95	205
	Dark Slate Blue	72	61	139

The background color of the object plane was chosen to be white so that the objects that will be focused are clearer in the scene. Fig. 8 presents the objects in 10 different colors, and Table II gives the decimal values of these colors. While selecting colors, it was made sure that each color component was different from zero (R≠0, G≠0, B≠0) and one of the color components was brighter than the others. The purpose here was to perform autofocusing using three different color components (R, G and B) and find which color component was more successful in focusing.

V. EXPERIMENTS

In this study, images for the objects containing the colors given in Table II and the patterns given in Fig. 7 were taken by using an RGB CCD camera. As it is seen in Fig. 8 and Table II, these images were divided into the three groups such that first, second and third groups contain only the images with dominant R, dominant G and dominant B, respectively. Every image from each group was divided into its R, G and B color components. Then each color component produced by this way was subjected to ASGA in order to obtain the following.

- To obtain the focusing accuracy on the R, G and B color components of the each color of each group (Dominant R, Dominant G and Dominant B),
- To determine the impact of the ASGA on the focusing accuracy depending on the values of the parameter k given in Table I.

In this study, we attempted to obtain the focusing error of the ASGA according to the dominant color components, i.e. to find the difference between the focusing found by ASGA and the actual focusing. Therefore, the ASGA was carried out on 600 different object fields belonging to groups given in Table II. The mean squared error (MSE) values for the ASGA were calculated using the following formula [19], [33].

$$MSE = \frac{1}{N}\sum_{y=1}^{N}(a_y - d_y)^2 \tag{8}$$

In this formula, N is the number of object fields where focusing has been done, a_y is the actual focusing, and d_y is the focusing obtained by the ASGA. As it is seen in Table III, the minimal error of the ASGA is achieved for the brightest component at k=2.

In Table IV, the ratio Q between the correct and incorrect focusing depending on the values of k is calculated using

(9). As it is seen in this Table, the maximum of ratio Q is achieved at k=2 as well (Table IV).

$$\text{ratio Q (\%)} = \frac{\text{Total number of correct autofocusing}}{\text{Total number of autofocus tests}}.100 \quad (9)$$

TABLE III. MSE VALUES OF ASGA CORRESPONDING TO EACH GROUP GIVEN IN TABLE II

Group	Color Comp.	MSE values			
		k=1	k=2	k=3	k=4
Dominant R	R	0,0005846	0,0000531	0,0004252	0,0004517
	G	0,0009965	0,0003587	0,0008769	0,0013951
	B	0,0011161	0,0003189	0,0008291	0,0011480
Dominant G	R	0,0006378	0,0003189	0,0004783	0,0005315
	G	0,0004769	0,0000399	0,0003762	0,0004937
	B	0,0007653	0,0003827	0,0006696	0,0007972
Dominant B	R	0,0034545	0,0001063	0,0018070	0,0021790
	G	0,0044244	0,0002790	0,0048629	0,0064573
	B	0,0011339	0,0000638	0,0012321	0,0019337

Considering the results in Table III and Table IV, it is seen that, the focusing performed using the brightest color component reveals higher performance.

TABLE IV. FOCUSING ACCURACY OF ASGA CORRESPONDING TO EACH GROUP GIVEN IN TABLE II

Group	Color Comp.	Ratio Q (%)			
		k=1	k=2	k=3	k=4
Dominant R	R	81,4	94,6	85,7	82,1
	G	70,0	85,0	82,5	72,5
	B	70,8	79,2	75,0	70,8
Dominant G	R	69,6	89,3	83,9	76,8
	G	72,5	95,0	85,0	90,0
	B	70,8	79,2	79,2	75,0
Dominant B	R	78,6	87,5	83,9	83,9
	G	80,0	80,0	72,5	72,5
	B	87,5	95,0	91,7	87,5

Based on these data, to increase the focusing accuracy of camera on RGB images we have prepared a MATLAB code which performs the PA based-BC focusing procedure given the details in the Section III. The pseudo code of the MATLAB code is given below.

```
Program Finding Focus

Begin

  1 Set the step progression of the lens to s=0.
  2 Take the RGB image.
  3 Calculate R̄, Ḡ, B̄ (Eq. 1,2,3).
  4 Assign as F thereof highest.
  5 Specify the image area to be focused on F.
  6 Take the image of the specified area.
  7 Calculate FV (Eq.7) using ASGA.
  8 If FVs-FVs-1 >= 0
              s=s+1
              go to 6.
  Else
      Accept FVs-1 as the optimum focus value.
      Assign s-1 as the optimum lens position.

  End
```

TABLE V. THE OVERALL FOCUSING PERFORMANCE OF PA BASED-BC FOR ALL OF RGB IMAGES

k	The overall MSE value	The overall Ratio Q (%) value
1	0,00073180	80,5
2	0,00005227	94,9
3	0,00067783	87,5
4	0,00095970	86,5

The above-mentioned code was applied to the total 600 focusing field having the features in Fig. 7 and Table II. Consequently, the results in Table IV were obtained. When these values are examined, it is seen that even if the brightness of the color components of the RGB image are changed, camera is able to focus with the overall focusing accuracy of 94,9% (Table V). The use of the PA based-BC for focusing of RGB camera has upgraded the focusing accuracy up to 95% for k=2 given in Table IV.

In this study, the resolutions of the smallest and the largest image fields where focusing has been done are 70x50 and 90x65, respectively. In result of the use of the above-mentioned pseudo code to find the FV of each image, for the smallest and the largest focusing fields it is determined that a time has passed between 43msn-108msn, respectively. As a result thereof, the duration of finding focus corresponds to a time between 0.8sn-2.2sn. If the embedded and integrated systems are used, this period may be even less.

VI. CONCLUSION

In this study the problem of autofocusing of RGB CCD camera is taken up. We conclude that focusing on an object to be photographed should be performed in two steps in order to solve the problem as sensitively as possible. In the first step, the image is divided into R, G and B components and the brightest of these components is chosen for focusing. In the second step, autofocusing is performed by ASGA in accordance with the contrast of the selected component. By the use of PA based-BC method which performs these procedures for focusing, the overall focusing accuracy of color camera was found as 94,9 (Table V).

REFERENCES

[1] R. Benes, P. Dvorak, M. Faundez-Zanuy, V. Espinosa-Duró, J. Mekyska, "Multi-Focus Thermal Image Fusion," Pattern Recognition Letters, vol. 34, no. 5, pp. 536-544, 2013. doi:10.1016/j.patrec.2012.11.011

[2] D. Wang, X. Ding, T. Zhang, H. Kuang, "A Fast Auto-Focusing Technique for the Long Focal Lens TDI CCD Camera in Remote Sensing Applications," Optics and Laser Technology, vol. 45, pp. 190-197, 2013. doi:10.1016/j.optlastec.2012.07.005

[3] J. Kautsky, J. Flusser, B. Zitova, S. Simberova, "A New Wavelet-Based Measure of Image Focus," Pattern Recognition Letters, vol. 23, no. 14, pp. 1785-1794, 2002. doi:10.1016/S0167-8655(02)00152-6

[4] S. Wu, W. Lin, L. Jiang, W. Xiong, L. Chen, "An Objective Out-Of-Focus Blur Measurement," Information, Communications and Signal Processing, 2005 Fifth International Conference on, pp. 334-338, 2005. doi:10.1109/ICICS.2005.1689062

[5] S. Pertuz, D. Puig, M. A. Garcia, "Reliability Measure for Shape-From-Focus," Image and Vision Computing, vol. 31, no. 10, pp. 725-734, 2013. doi:10.1016/j.imavis.2013.07.005

[6] C. Y. Chen, R. C. Hwang, Y. J. Chen, "A Passive Auto-Focus Camera Control System," Applied Soft Computing, vol. 10, no. 1, pp. 296-303, 2010. doi:10.1016/j.asoc.2009.07.007

[7] S. H. Jin, J. U. Cho, J. W. Jeon, "FPGA Based Passive Auto Focus System Using Adaptive Thresholding," in Proceedings of SICE-ICASE International Conference, pp. 2290-2295, 2006. doi:10.1109/SICE.2006.315356

[8] J. Widjaja, S. Jutamulia, "Wavelet Transform-Based Autofocus Camera Systems," in Proceedings of The 1998 IEEE Asia-Pacific Conference on Circuits and Systems, pp. 49-51, 1998. doi:10.1109/APCCAS.1998.743655

[9] I. H. Lee, S. O. Shim, T. S. Choi, "Improving Focus Measurement via Variable Window Shape on Surface Radiance Distribution for 3D Shape Reconstruction," Optics and Lasers in Engineering, vol. 51, no. 5, pp. 520–526, 2013. doi:10.1016/j.optlaseng.2012.11.003

[10] E. Turgay, O. Teke, "Autofocus Method in Thermal Cameras Based on Image Histogram," 2011 IEEE Conference on 19th Signal Processing and Communications Applications, pp. 462-465, 2011. doi:10.1109/SIU.2011.5929687

[11] S. B. Roh, S. K. Oh, W. Pedrycz, K. Seo, "Development of Autofocusing Algorithm Based on Fuzzy Transforms," Fuzzy Sets and Systems, vol. 288, pp. 129-144, 2016. doi:10.1016/j.fss.2015.08.029

[12] C. Zhou, X. Hu, Y. Zhou, "An Induced Fluorescence Detecting System with Autofocus Electrically Tunable Len", IACSIT International Journal of Engineering and Technology, vol. 8, no. 4, pp. 297-300, 2016. doi:10.7763/IJET.2016.V8.901

[13] Y. Zhang, Y. Zhang, C. Wen, "A New Focus Measure Method Using Moments," Image and Vision Computing, vol. 18, no. 12, pp. 959-965, 2000. doi:10.1016/S0262-8856(00)00038-X

[14] M. Subbarao, J. K. Tyan, "Selecting the Optimal Focus Measure for Autofocusing and Depth-From-Focus," IEEE Transactions on Pattern Analysis and Machine Intelligence, vol. 20, no. 8, pp. 864-870, 1998. doi:10.1109/34.709612

[15] W. Huang, Z. Jing, "Evaluation of Focus Measures in Multi-Focus Image Fusion," Pattern Recognition Letters, vol. 28, no. 4, pp. 493-500, 2007. doi:10.1016/j.patrec.2006.09.005

[16] L. Fan, F. Song, S. Jutamulia, "Edge Detection with Large Depth of Focus Using Differential Haar–Gaussian Wavelet Transform," Optics Communications, vol. 270, no. 2, pp. 169-175, 2007. doi:10.1016/j.optcom.2006.09.015

[17] D. M. Tsai, C. C. Chou, "A Fast Focus Measure for Video Display Inspection," Machine Vision and Applications, vol. 14, no. 3, pp. 192-196, 2003. doi:10.1007/s00138-003-0126-1

[18] H. C. Chang, T. M. Shih, N. Z. Chen, N. W. Pu, "A Microscope System Based on Bevel-Axial Method Auto-Focus," Optics and Lasers in Engineering, vol. 47, no. 5, pp. 547-551, 2009. doi:10.1016/j.optlaseng.2008.10.004

[19] M. Selek, "An Adaptive Squared Gradient Algorithm for Autofocusing of Thermal Cameras," International Journal of Innovative Computing Information and Control, vol. 9, no. 2, pp. 841-849, 2013.

[20] I. Lee, M. T. Mahmood, T. S. Choi, "Adaptive Window Selection for 3D Shape Recovery from Image Focus," Optics and Laser Technology, vol.45, pp. 21-31, 2013. doi:10.1016/j.optlastec.2012.08.003

[21] M. G. Chun, S. G. Kong, "Focusing in Thermal Imagery Using Morphological Gradient Operator," Pattern Recognition Letters, vol. 38, pp. 20-25, 2014. doi:10.1016/j.patrec.2013.10.023

[22] O. Lossona, L. Macairea, Y. Yanga, "Comparison of Color Demosaicing Methods," Advances in Imaging and Electron Physics, vol. 162, pp. 173-265, 2010. doi:10.1016/S1076-5670(10)62005-8

[23] P. M. Hubel, J. Liu, R. J. Guttosch, "Spatial Frequency Response of Color Image Sensors: Bayer Color Filters and Foveon X3," Sensors and Camera Systems for Scientific, Industrial and Digital Photography Applications V Proc. SPIE, vol. 5301, pp. 402-407, 2004. doi:10.1117/12.561568

[24] X. Li, B. Gunturk, L. Zhang, "Image Demosaicing: a Systematic Survey," Visual Communications and Image Processing Proceedings SPIE, vol. 6822, 2008. doi:10.1117/12.766768

[25] Z. Sadeghipoor, Y.M. Lu, S. Süsstrunk, "Optimum Spectral Sensitivity Functions for Single Sensor Color Imaging," in Proceedings of SPIE Conference on Digital Photography VIII, vol. 8299, 2012. doi:10.1117/12.907904

[26] X. Xu, Y. Wang, J. Tang, X. Zhang, X. Liu, "Robust Automatic Focus Algorithm for Low Contrast Images Using a New Contrast Measure," Sensors, vol. 11, pp. 8281-8294, 2011. doi:10.3390/s110908281

[27] S. Podlech, "Autofocus by Bayes Spectral Entropy Applied to Optical Microscopy," Microscopy and Microanalysis, pp. 1-9, 2016. doi:10.1017/S1431927615015652

[28] R. O. Panicker, B. Soman, G. Saini, J. Rajan, "A Review of Automatic Methods Based on Image Processing Techniques for Tuberculosis Detection from Microscopic Sputum Smear Images," Journal of Medical Systems, vol. 40, pp. 1-13, 2016. doi:10.1007/s10916-015-0388-y

[29] X. Zhang, H. Wu, Y. Ma, "A New Auto-Focus Measure Based on Medium Frequency Discrete Cosine Transform Filtering and Discrete Cosine Transform," Applied and Computational Harmonic Analysis, vol. 40, pp. 430-437, 2016. doi:10.1016/j.acha.2015.08.008

[30] X. Zuojiang, H. Di, Z. Haibin, W. Liang, X. Zhigang, "Research on Automatic Focusing Technique Based on Image Autocollimation," Optik-International Journal for Light and Electron Optics, vol. 127, pp. 148-151, 2016. doi:10.1016/j.ijleo.2015.10.037

[31] B. Neumann, A. Dämon, D. Hogenkamp, E. Beckmann, J. Kollmann, "A Laser-Autofocus for Automatic Microscopy and Metrology," Sensors and Actuators, vol. 17, no. 1-2, pp. 267-272, 1989. doi:10.1016/0250-6874(89)80090-3

[32] N. Kehtarnavaz, H. J. Oh, "Development and Real-Time Implementation of A Rule-Based Auto-Focus Algorithm," Real-Time Imaging, vol. 9, pp. 197-203, 2003. doi:10.1016/S1077-2014(03)00037-8

[33] M. Gamadia, N. Kehtarnavaz, K. Roberts-Hoffman, "Low-Light Auto-Focus Enhancement for Digital and Cell-Phone Camera Image Pipelines," IEEE Transactions on Consumer Electronics, vol. 53, no. 2, 2007. doi:10.1109/TCE.2007.381682

[34] S. Y. Lee, J. T. Yoo, Y. Kumar, S. W. Kim, "Reduced Energy-Ratio Measure for Robust Autofocusing in Digital Camera," IEEE Signal Processing Letters, vol. 16, no. 2, pp. 133-136, 2009. doi:10.1109/LSP.2008.2008938

[35] H. D. Cheng, X. H. Jiang, Y. Sun, J. Wang, "Color Image Segmentation: Advances And Prospects," Pattern Recognition, vol. 34, pp. 2259-2281, 2001. doi:10.1016/S0031-3203(00)00149-7

[36] F. C. A. Groen, I. T. Young, G. Ligthart, "A Comparison of Different Focus Functions for Use in Autofocus Algorithms," Cytometry, vol. 6, pp. 81-91, 1985. doi:10.1002/cyto.990060202

[37] J. W. Han, J. H. Kim, H. T. Lee, S. J. Ko, "A Novel Training Based Auto-Focus for Mobile-Phone Cameras," IEEE Transactions on Consumer Electronics, vol. 57, no. 1, pp. 232–238, 2011. doi:10.1109/TCE.2011.5735507

[38] S.Y. Lee, Y. Kumar, J. M. Cho, S. W. Lee, S. W. Kim, "Enhanced Autofocus Algorithm Using Robust Focus Measure and Fuzzy Reasoning," IEEE Transactions on Circuits and Systems for Video Technology, vol. 18, no. 9, pp. 1237–1246, 2008. doi:10.1109/TCSVT.2008.924105

[39] J. Lee, K. Kim, B. Nam, "Implementation of a Passive Automatic Focusing Algorithm for Digital Still Camera," IEEE Transactions on Consumer Electronics, vol. 41, no. 3, pp. 449-454, 1995. doi:10.1109/30.468047

[40] Y. Sun, S. Duthaler, B. J. Nelson, "Autofocusing in Computer Microscopy: Selecting The Optimal Focus Algorithm," Microscopy Research and Technique, vol. 65, no. 3, pp. 139–149, 2004. doi:10.1002/jemt.20118

[41] M. Kristan, J. Pers, M. Perse, S. Kovacic, "A Bayes-Spectral-Entropy-Based Measure of Camera Focus Using a Discrete Cosine Transform," Pattern Recognition Letters, vol. 27, pp. 1431–1439, 2006. doi:10.1016/j.patrec.2006.01.016